ACADEMIA ROMÂNĂ
Revue Roumaine de Chimie
http://web.icf.ro/rrch/

Rev. Roum. Chim.,
2018, *63*(4), 287-292

SYNTHESIS AND CHARACTERIZATION OF ZnO NANOPARTICLES FOR PHOTOCATALYTIC REMOVAL OF PHENOL FROM WATER

Ahmed A. ABD ELRAADY,[a] Gaber H. G. AHMED[b*] and Fawzy H. ASSAF[a]

[a] Chemistry Department. Faculty of Science, South Valley University, Qena, 83523 Egypt
[b] Chemistry Department, Faculty of Science, Damanhur University, Damanhour, 22511, Egypt

Received August 19, 2017

Easy synthesis was performed for ZnO nanoparticles by precipitation method followed by its calcination in atmospheric oxygen at a temperature range 400-550°C for 2 h. XRD, TEM, SEM, BET surface area and UV-vis spectroscopy analyses were utilized for ZnO characterization. The as-synthesized ZnO nanoparticles showed high photocatalytic efficiency for the removal of aqueous phenol comparing with direct photolysis using UV radiation. ZnO calcined at 400°C (ZnO-400) has an average crystallite size of about 43 nm and a particle size range 15-40 nm according to XRD and TEM analyses, respectively. It has a hexagonal wurtzite structure with an estimated optical band gap energy of 3.17 eV from spectrophotometric analysis. The BET surface area decreases from: 13.8 m^2/g to 8.34 m^2/g with increasing calcination temperature from 400 ºC to 550 ºC.

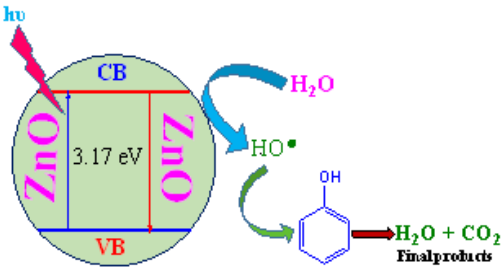

INTRODUCTION

Semiconductor nanoparticles have gotten impressive considerations since a few decades ago because of their basic arrangement, controllable size, morphological tunability, novel physical and chemical properties, simple functionalization, and more extensive applications such as solar cells, electroluminescent devices, electrochromic windows and chemical sensors.[1,2] The metal oxides utilized within these applications are obliged to have a high surface area in addition to great electrical, electrochemical and structural properties.

Among them, ZnO is a versatile material with multifunctional properties that has a wide band gap (3.3 eV) with a substantial exciton binding energy of 60 meV at room temperature,[2] has high chemical stability, high electrochemical coupling coefficient, broad range of radiation absorption and high photostability.[3] It has been utilized within gas sensors, optoelectronics, photovoltaic applications, photocatalytic oxidation, sun-based cells and analytical sensing.[4-7] Also, it has been included in different industries like rubber, pharmaceutical, cosmetics, textile, electronics and electrotechnology, and other industries.[1,3,8] Moreover, different qualities of novel nanostructures of ZnO have been effectively integrated through numerous synthetic routes, for example, nanowires, nanobelts, and nanotetrapods.[1]

Using of photocatalytic methods as a technology for water treatment is rapidly developing.[9,10] These photocatalytic methods are capable of decomposing organic pollutants in the aqueous media and may lead finally to their mineralization. However, adoption of an appropriate treatment method depends on some factors like the nature of the pollutant, its concentration, the efficiency of treatment method and its economic cost, etc. Various characteristics of the photocatalysts can be controlled by controlling the different preparation conditions like the precursor,

* Corresponding author: gaber.ahmed@damanhour.edu.eg, Tel:+201202908599

the calcination temperatures, the pH and doping with different cations and anions.[11-17]

Phenol and its derivatives exhibit acute toxicity and emerge to the environment through various natural and industrial sources.[18] Leached phenol gives ground and surface waters unpleasant odor and taste. Although, phenol is a refractory organic pollutant to the normal treatment techniques, photocatalysis method was used effectively to remove phenol from aqueous environments.[19-21] Therefore, mineralization of phenol by new, effective, and inexpensive methods is an environmental demand. ZnO is a cheap semiconductor material and is known to have high photocatalytic efficiency under UV and sunlight irradiation.[18,22,23] Herein, we synthesized ZnO nanoparticles photcatalyst by the precipitation method followed by its calcination in atmospheric oxygen at the temperature range 400-550°C. Different analytical and microscopic techniques were used to characterize ZnO nanoparticles that were used adequately for phenol removal from water under UV irradiation.

RESULTS AND DISCUSSION

ZnO was prepared by means of sol-gel technique by different authors and utilized viably for the photocatalytic oxidation of phenol.[20,24] However, sol-gel integrated ZnO contains adsorbed water and might be a better choice in case of further surface functionalization *via* covalent bonding with adsorbed OH groups. In our study, we favored calcination of ZnO so as to acquire dry and stable nanoparticles.

The following Miller indices: (1 0 0), (0 0 2), (1 0 1), (1 0 2), (1 1 0), (1 0 3), (2 0 0), (1 1 2), and (2 0 1) were observed in Figure 1, which are consistent with (JCPDS card No. 36–1451) indicating the formation of hexagonal wurtzite ZnO structure for the dried precipitate.

Characterization of the as-synthesized ZnO powder

Figures (2a) and (2b) show the XRD patterns of ZnO calcined at 400 °C and 550 °C, respectively. A series of nine intense characteristic peaks related to the corresponding Miller indices (1 0 0), (0 0 2), (1 0 1), (1 0 2), (1 1 0), (1 0 3), (2 0 0), (1 1 2), and (2 0 1), are observed for both samples. These peaks are consistent with the standard pattern of hexagonal wurtzite ZnO structure and match well with the JCPDS data [JCPDS # 36-145]. These results demonstrate the good crystallinity of the synthesized ZnO samples in addition to the absence of impurities (high purity). Also, the ZnO structure is not changed or affected after calcination. Using K=0.9 for hexagonal structures, the average crystallite size was calculated from XRD analysis using the Scherrer equation (eqn. 1) to be 43.12 nm and 44.99 nm for ZnO-400 and ZnO-550, respectively.

$$\tau = \frac{K\lambda}{\beta\cos\theta} \qquad (1)$$

where (τ) is the crystallite size, (λ =1.5405 Å) is the x-ray wavelength, (β) is the line broadening at half the maximum intensity (FWHM) in radians, (θ) is the Bragg angle, and (K) is the shape factor and its value interchangeable dependent on the shape of crystallites, from 0.89 for spherical to 0.94 for cubic particles.

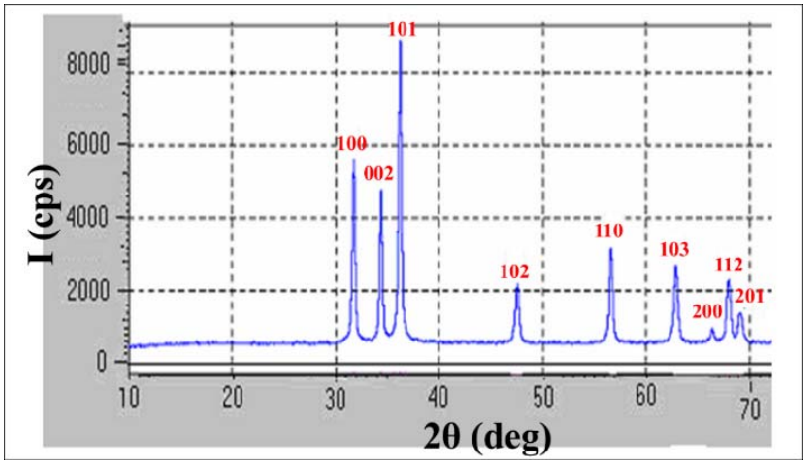

Fig. 1 – XRD pattern of the dry precipitate obtained before calcination and after the drying step at 140°C.

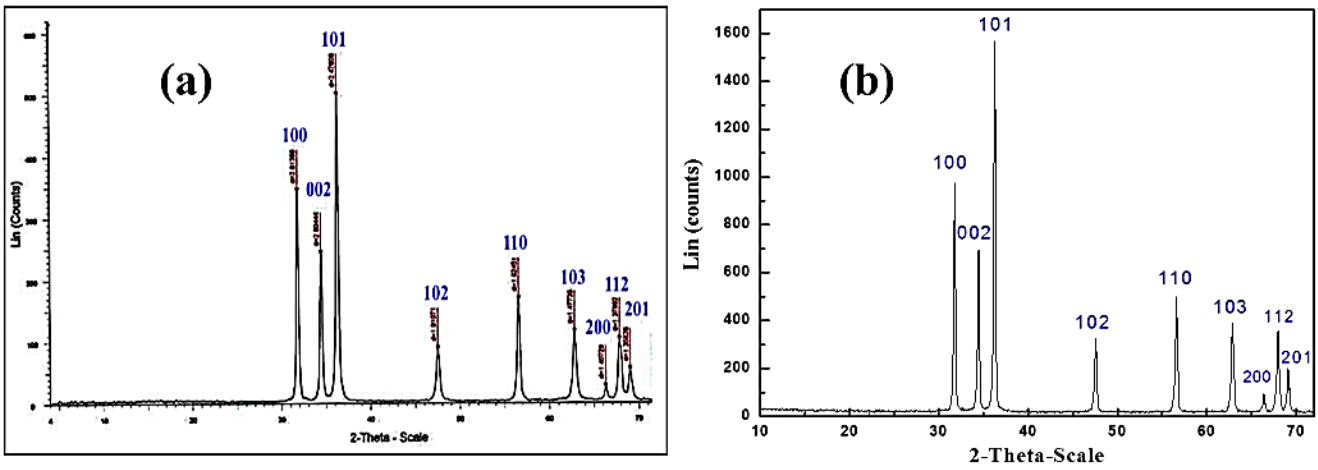

Fig. 2 – XRD pattern of (a) ZnO-400 and (b) ZnO-550.

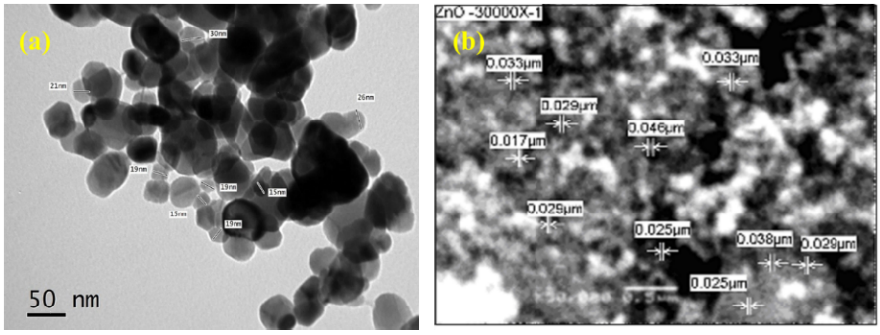

Fig. 3 – (a) TEM image of ZnO-400 (b) SEM image of ZnO-400.

Figures 3(a) and 3(b) show the TEM and SEM images of ZnO calcined at 400 ºC. These figures confirm the homogeneous nature of ZnO surface. It is also clear that ZnO particles are mostly aggregated and consist of nearly hexagonal grains of uniform shape in the nanoscale which is consistent with the XRD results. Also, the values of the particle size given in Figure 3(a) are in complete accordance with the mean crystallite size calculated from the XRD analysis for the same sample. The SEM image of the same ZnO sample is given in figure 3(b). This figure confirms the homogeneity of ZnO surface.

The UV-vis spectrum of ZnO-400 is given in figure 4(a). The value of the onset wavelength (λ) of absorption was determined to be 418 nm. The corresponding band gap was calculated from the following equation (eqn.2):[20]

$$E_g = \frac{1240}{\lambda(nm)} \tag{2}$$

where 1240 is a constant which equals hc, h is Plank's constant (6.626 x10^{-34} J s), c is the speed of light (2.998 x 10^8 m.s^{-1}), and λ is the cutoff wavelength at 418 nm. The calculated value of the band gap using this equation is 2.97 eV. This value is slightly smaller than in the literature and this may be explained due to the slight increase of the ZnO particle size.

Another way to estimate the band gap energy is to calculate the absorption coefficient (α) which is related to the length of the absorption media (thickness of cell) and absorbance by the following relation (eqn.3):[25]

$$\alpha = 2.303\left(\frac{A}{L}\right) \tag{3}$$

where α is the absorption coefficient, A is the absorbance, and L is the thickness of the cell and equal unity in this case. This method is most abundant for thin-film manufactured ZnO and the optical band gap could be calculated, assuming an indirect allowed transition, using Tauc equation (eqn.4):[25]

$$(\alpha h\nu)^2 = C\left(h\nu - E_g\right) \tag{4}$$

where C is constant and $h\nu$ is the incident photon energy. A plot of $(\alpha h\nu)^2$ *vs* hν is shown in Figure 4(b), E_g is estimated to be 3.17 eV by extrapolating the straight line to αhν = 0. This value is in agreement with the previous value.

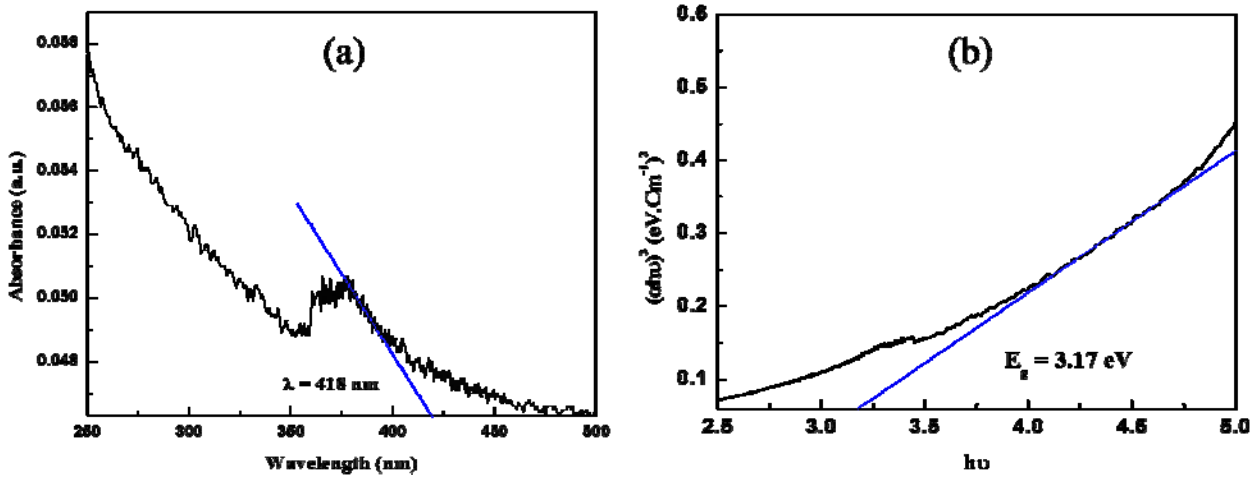

Fig. 4 – (a) UV–Vis spectra of calcined ZnO powder at 400°C
(b) The indirect allowed transition calculated optical energy band gap for ZnO-400.

The three ZnO samples (calcined at 400, 450 and 550°C) were outgassed at 200 °C for 1 h prior to BET surface area measurements. The values of BET were found to be 13.8, 13.7 and 8.34 m^2/g for samples calcined at 400, 450 and 550°C, respectively. This indicates the decrease of BET surface area with increasing calcination temperatures and this could be explained due to the increase of the particle size as indicated by XRD analysis. The above results show that ZnO-400, which exhibited the highest surface area among others, could be used effectively as a photocatalyst for phenol removal.

Photocatalytic activity of ZnO nanoparticles

In these experiments ZnO-400 was used as the photocatalyst for phenol removal from water. The phenol solution was left in contact with air because oxygen plays an important role in the photocatalytic process.[26] In addition it was stirred using a magnetic stirrer for a better contact between the photocatalyst and the aqueous solution.

Preliminary experiments (at similar experimental conditions but in the absence of the radiation source) showed that less than 6% of phenol was removed after 17 hours of stirring. No intermediates were found in HPLC chromatogram suggesting that the decrease of phenol concentration is attributable to an adsorption process only.

Figure 5 shows the removal of phenol by direct photolysis using UV radiation alone and by UV in the presence of ZnO nanoparticles. The reaction is fast in the first hours then the rate decreases gradually. It is clear that ZnO/UV have higher efficiency for phenol removal than UV alone. Removal of phenol by UV alone may be due to the formation of hydroxyl radical in the presence of O_2.[26] Formation of a polymer was also suggested to explain the removal of phenol by UV direct photolysis.[27] The enhancement of the rate of phenol removal in the presence of ZnO photocatalyst may be attributed to the formation of hydroxyl radical resulting from the reduction of oxygen or water. It is noteworthy that catechol, hydroquinone and resorcinol were detected as removal products beside short chain carboxylic acids as shown in Figure 5 (1S, Electronic Supplementary Information (ESI). Carbon Oxygen Demand (COD) test can be used to quantify the amount of organics in water. We used this test to examine the efficiency of the prepared ZnO for further decomposition of the products formed due to phenol removal. For this purpose a 300 mL phenol (initial COD is 53.9 mg/L) was treated in the presence of UV and 300 mg of ZnO. After 24 hrs of treatment the COD was decreased to 6.5 mg/L. This result indicates that ZnO is efficient for the decomposition of the products formed during phenol photo degradation under the experimental conditions used.

The photocatalytic activity of the as-synthesized ZnO was also tested with another small organic pollutant, formic acid, and in the presence of sunlight. The results, discussed in details in ESI, indicate that ZnO could be used efficiently for other organic pollutants. Also, it could be used at a wide range of wavelengths in addition to direct sunlight.

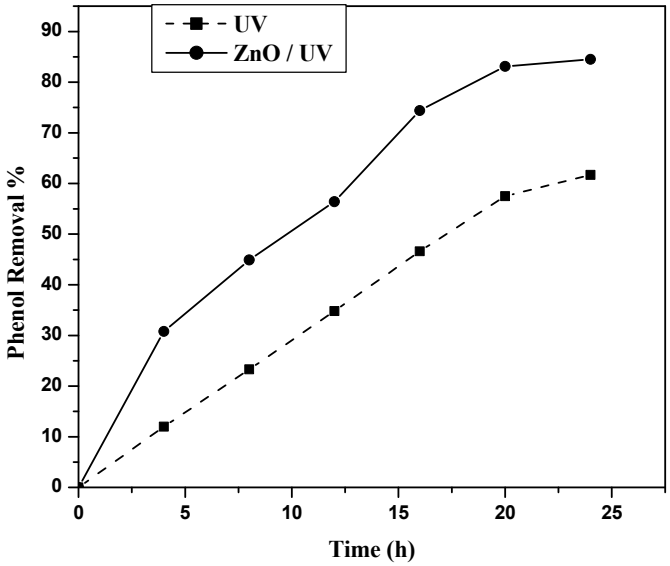

Fig. 5 – Removal of phenol by UV and ZnO/UV.
Phenol conc. = ($1x10^{-3}$ M), λ=330 nm and the reaction temperature changed from 26 to 37ºC.

EXPERIMENTAL

Preparation of ZnO photocatalyst

ZnO has been prepared as follows: 11 g of zinc acetate dihydrate were dissolved in a mixture of 20 mL distilled water and 20 mL absolute ethanol. While the solution was subjected to vigorous stirring and a temperature of 70°C, a basic aqueous solution of ammonium bicarbonate (NH_4HCO_3) and ammonium carbamate (NH_2COONH_4) mixture of equal weights was added slowly to this solution till complete precipitate. The precipitate was filtered off, washed well by ethanol and distilled water, dried at 140°C in an oven and then it was calcined in a muffle furnace, in air, at different temperatures (400, 450 and 550°C) for 2 hrs.

Method and apparatus

All experiments were carried out in a semi-batch apparatus using 500 mL Pyrex glass beaker. 400 mL of distilled water containing 1 mM of phenol in addition to 500 mg of the catalyst were irradiated using a UV irradiation lamp (Philips, maximum intensity at λ = 330 nm). The beaker was held at a fixed distance under the UV lamp in a small box, the interior walls of which were covered by aluminum foil. In all photocatalytic experiments, the solutions were stirred using a MSH-20A hotplate stirrer with the same stirring speed in each experiment. The temperature was measured using a thermometer and the beaker was covered with glass watch in order to prevent the mechanical loss of solution.

Instrumentation

An x-ray diffractometer model (Shimadzu, XRD-7000, Japan) with Ni filtered Cu Kα radiation (λ=1.5418 Å) was used to characterize the formed precipitate before calcinations and a diffractometer model (Brucker Axs-D8 Advance) (using Manual DIFFRAC Plus EVA 2001 method) was used for the identification of ZnO after calcination. The crystallite size was calculated from the XRD results using the Scherrer equation (eqn.(1)).

Transmission electron microscope (TEM) instrument model (Jeol JEM-1230 Electron Microscope, 120 kv, Japan) was used for the determination of particle size as well as the shape for ZnO-400.

The surface morphology of ZnO-400 sample was investigated using the scanning electron microscope, (SEM) (Jeol, JSM-636DLA, Japan).

Ultraviolet-Visible spectrophotometer model (Shimadzu 2460, Japan) was used for the determination of the onset wavelength (λ) of absorption for the ZnO sample calcined at 400 ºC.

The specific surface areas of the different catalysts were calculated using the BET method from the nitrogen adsorption isotherm of the calcined samples at the liquid nitrogen temperature, *ca.* -196°C, using an automatic ASAP 2010 Sorptometer, Micromeretics, USA.

Analysis

Phenol and its degradation products were analyzed by High Performance Liquid Chromatograph (HPLC, PERKIN-ELMER model 1022 LC). Detection was carried out at 210 nm with a 785A UV-Vis detector. The chromatograph was supplied with a Supel Cosil LC -18 column (15cm x 4.6 mm x 5 µm). A mixture of water, acetonitrile and H_3PO_4 (89.9: 10: 0.1 by volume, respectively) with a flow rate of 1 ml\min was used as an eluent. Samples were analyzed by HPLC immediately after centrifugation. All samples were analyzed 3 times and the average peak area was calculated. The concentration of a compound was calculated using a calibration curve.

COD is a measure of the amount of oxygen that is consumed by a reaction in a given solution and is expressed in mass of oxygen consumed over a certain volume of solution (mg/L). COD was measured by filterphotometer (LOVIBOND, Germany) using the dichromate/H_2SO_4 method.

CONCLUSIONS

ZnO nanoparticles were synthesized successfully by a precipitation method followed by its calcination,

in air, at 400-550ºC for 2 hrs. The resulting ZnO nanoparticles were characterized by different techniques and were used for the removal of phenol from water. ZnO/UV exhibited higher photocatalytic efficiency for phenol removal from aqueous media than direct photolysis by UV alone thanks to the higher rate of hydroxyl radical formation. ZnO nanoparticles calcined at 400°C has the highest efficiency among others obtained at higher temperatures mainly due to their smaller size and higher surface area. ZnO-400 was found also photocatalytically active with other organic pollutant, formic acid, and under different irradiation sources including sunlight.

REFERENCES

1. D. Liu, W. Wu, Y. Qiu, S. Yang, S. Xiao, Q. Wang and L. Ding, *Langmuir*, **2008**, *24*, 5052. DOI: 10.1021/la800074f
2. Z. L. S. Seow, A. S. W. Wong, V. Thavasi, R. Jose, S. Ramakrishna and G.W. Ho, *Nanotechnology*, **2009**, *20*, 045604. https://doi.org/10.1088/0957-4484/20/4/045604
3. A. K. Radzimska and T. Jesionowski, *Materials*, **2014**, *7*, 2833. doi:10.3390/ma7042833
4. X. Jin, Y. X. Li, Y. Su, Z. Guo, C. P. Gu, J. R. Huang, F. L. Meng, X. J. Huang, M. Q. Li and J. H. Liu, *Nanotechnology*, **2016**, *27*, 355702. doi:10.1088/0957-4484/27/35/355702
5. R. Rathnasamy, P. Thangasamy, R. Thangamuthu, S. Sampath and V. Alagan, *J. of Mat. Sc.: Materials in Electronics*, **2017**, *28*, 10374–10381. https://doi.org/10.1007/s10854-017-6807-8
6. M. H. Jung, *Mater. Chem. Phys.*, **2017**, *202*, 234-244. https://doi.org/10.1016/j.matchemphys.2017.09.034
7. S. K. Basha, K. V. Lakshmi and V. S. Kumari, *Sensing and Bio-Sensing Research*, **2016**, *10*, 34-40. https://doi.org/10.1016/j.sbsr.2016.08.007
8. S. Mansouria, R. Bourguigaa and F. Yakuphanoglu, *Curr. Appl. Phys.*, **2012**, *12*, 1619. https://doi.org/10.1016/j.cap.2012.05.039
9. J. Krýsa, G. Waldner, H. M. ánková, J. Jirkovský and G. Grabner, *App. Cat. B: Env.*, **2006**, *64*, 290. https://doi.org/10.1016/j.apcatb.2005.11.007
10. D. Bahnemann, *Solar Energy*, **2004**, *77*, 445-452. https://doi.org/10.1016/j.solener.2004.03.031
11. L. Wang and M. Muhammed, *J. Mater. Chem.*, **1999**, *9*, 2871. DOI**:**10.1039/A907098B
12. A. Bagabas, A. Alshammari, M. Aboud and H. Kosslick, *Nanoscale Res. Lett.*, **2013**, *8*, 516. https://doi.org/10.1186/1556-276X-8-516
13. S. Musić and A. Šarić, *Ceramics Int.*, **2012**, *38*, 6047-6054. https://doi.org/10.1016/j.ceramint.2012.04.020
14. X. Junli, C. Ya, H. Yide, H. Men and Z. Xia, *RSC Adv.*, **2016**, *6*, 96778-96784. DOI: 10.1039/C6RA19622E
15. C. P. Rezende, J. B. da Silva and N. D. S. Mohallem, *Brazilian J. of Physics*, **2009**, *39*, 248-256. http://www.sbfisica.org.br/bjp/files/v39_248.pdf
16. Y. Wanga, C. Zhangb, S. Bib and G. Luo, *Powder Technol.*, **2010**, *202*, 130-139. https://doi.org/10.1016/j.powtec.2010.04.027
17. N. Shakti and P. S. Gupta, *Appl. Physics Res.*, **2010**, *2*, 19-24. DOI: http://dx.doi.org/10.5539/apr.v2n1p19
18. P. R. Shukla, S. Wang, H. M. Ang and M. O. Tadé, *Sep. and Pur. Tech.*, **2010**, *70*, 338-347. https://doi.org/10.1016/j.seppur.2009.10.018
19. J. Jingjing, W. Hongtao, C. Xiaodong, L. Shuo, X. Tengfeng, W. Dejun and L. Yanhong, *J. of Coll. Int. Sci.*, **2017**, *494*, 130–138. https://doi.org/10.1016/j.jcis.2017.01.064
20. H. Benhebal, M. Chaib, T. Salmon, J. Geens, A. Leonard, S. D. Lambert, M. Crine and B. Heinrichs, *Alexandria Eng. J.*, **2013**, *52*, 517-526. https://doi.org/10.1016/j.aej.2013.04.005
21. S. J. Darzi and M. Movahedi, *Iran. J. Chem. Chem. Eng.*, **2014**, *33*, 55. http://www.ijcce.ac.ir/article_10756_beddc19a112915076294ee413d7f35ae.pdf
22. M. M. Ba-Abbad, A. H. Kadhum, A. Mohamad, M. S. Takriff and K. Sopian, *Int. J. Thermal Environ. Eng.,* **2010**, *1*, 37. DOI: 10.5383/ijtee.01.01.006
23. H. Dewidar, S. A. Nosier and A.-H. El-Shazly, *J. Chem. Health Safety*, **2017**, https://doi.org/10.1016/j.jchas.2017.06.001.
24. I. Prabha and S. Lathasree, *Mat. Sc. Semiconductor Processing*, **2014**, *26*, 603-614. https://doi.org/10.1016/j.mssp.2014.05.031
25. W. R. Saleh, N. M. Saeed, W. A. Twej and M. Alwan, *Adv. Mat. Phys. Chem.*, **2012**, *2*, 11-18. DOI: 10.4236/ampc.2012.21002
26. C. Wu, X. Liu, D. Wei, J. Fan and L. Wang, *Wat. Res.*, **2001**, *35*, 3927-3934. https://doi.org/10.1016/S0043-1354(01)00133-6
27. H. Chun, W. Yizhong and T. Hongxiao, *Chemosphere*, **2000**, *41*, 1205-1216. https://doi.org/10.1016/S0045-6535(99)00539-1